Available online at www.sciencedirect.com
SCIENCE DIRECT
Tetrahedron
Tetrahedron 62 (2006) 2779–2788

# A coordinatively unsaturated ruthenium methoxide as a highly effective catalyst for the halogen atom-transfer radical cyclization of *N*-allyl dichloroacetamides and related reactions

Yukihiro Motoyama, Shiori Hanada, Kazuya Shimamoto and Hideo Nagashima*

*Graduate School of Engineering Science, Institute for Materials Chemistry and Engineering, Kyushu University, Kasuga, Fukuoka 816-8580, Japan*

Received 30 November 2005; revised 29 December 2005; accepted 6 January 2006

Available online 7 February 2006

**Abstract**—Atom-transfer radical cyclization (ATRC) catalyzed by coordinatively unsaturated ruthenium alkoxides **4**, $[(\eta^5\text{-}C_5Me_5)\text{-}Ru(OR)]_2$, is investigated, and ruthenium methoxide **4a** (R = Me) is found to exhibit excellent catalytic activity for the cyclization of *N*-allyl-α,α-dichloroacetamides at ambient temperature. Addition of some amounts of two-electron donor ligands such as pyridine and triphenylphosphine improves the catalyst efficiency to afford the corresponding γ-lactams in high yields. The high catalytic activity of this catalyst system enables to control the diastereoselectivity of this 5-*exo* cyclization kinetically. The present **4a**/pyridine system is also effective for the 4-*exo* cyclization of *N*-vinylacetamides to afford the corresponding β-lactams in quantitative yields. The **4a**/pyridine system is also active towards the ATRP of methyl methacrylate (MMA) at room temperature to afford the poly(MMA) with narrow molecular weight distributions ($M_w/M_n = 1.2$) at the initial stage.


## 1. Introduction

Atom-transfer radical reaction (ATRR) has now become one of the most important carbon–carbon bond-forming reactions, being utilized for synthetic organic chemistry and polymer synthesis.[1–3] In particular, our discovery of copper-catalyzed cyclizations of allyl α,α,α-trichloroacetates[4a] and *N*-allyl-α,α,α-trichloroacetamides[4b] offered a research field of transition metal-catalyzed atom-transfer radical cyclization (ATRC), which has afforded powerful synthetic methods for carbo- and heterocycles including macrolide and alkaloid skeletons.[5] From the synthetic point-of-view, it should be noted that requirement of high reaction temperatures is a general disadvantage of ATRR, especially in the reactions involving activation of less reactive carbon–halogen bonds. In our earliest report on the cyclization of α-halogenated *N*-allylacetamides, either $RuCl_2(PPh_3)_3$ or CuCl catalyst was effective at 140 °C.[4b] Later elaboration to improve the reaction conditions revealed that the reaction was facilitated by increasing the halogen atom at the α-position and/or introduction of electron-withdrawing group on the nitrogen atom.[4e,f] This is presumably due to the fact that these substituents lower the LUMO of α-halogenated acetyl moiety and facilitate abstraction of a halogen atom by transition metal catalysts. On the other hand, several reactive catalyst systems, which can promote the reaction at low temperature, were developed; in particular, catalyst systems composed of CuCl and bidentate diamines[4c] and isolable coordinatively unsaturated ruthenium amidinates **1**–**3** were found to be one of the most effective catalysts for ATRR (Fig. 1).[6c,7] Thus, combination of the selection of appropriate substrates, which have suitable electronic structures for ATRR, with powerful catalyst systems realized the cyclization of *N*-allyl-α,α,α-trichloroacetamides below room temperature within a few hours. However, the cyclization of less reactive substrates such as *N*-allyl-α,α-dichloroacetamides is slow even using CuCl/bipyridine and ruthenium amidinates as the catalyst and it is necessary to apply high reaction temperatures (>80 °C) to obtain the product in good yield.[4e,7,8] This indicates the requirement to seek for catalysts more powerful enough to activate a carbon–chlorine bond of *N*-allyl dichloroacetamides with ease to afford the corresponding γ-lactams.

For the development of highly reactive new catalysts, we have been interested in use of coordinatively unsaturated transition metal complexes. ATRC is generally explained by the catalytic cycle shown in Scheme 1. The atom-transfer

*Keywords*: Coordinatively unsaturated complex; Polymerization; Radical cyclization; Ruthenium.
* Corresponding author. Tel.: +81 92 583 7819; fax: +81 92 583 7819; e-mail: nagasima@cm.kyushu-u.ac.jp

0040–4020/$ - see front matter © 2006 Elsevier Ltd. All rights reserved.
doi:10.1016/j.tet.2006.01.011

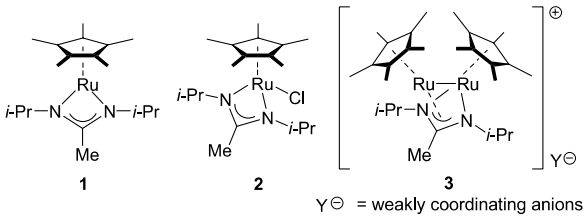


**Figure 1.** Ruthenium amidinate complexes **1**–**3**.

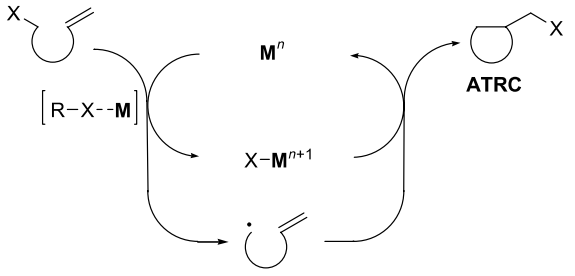


**Scheme 1.** Atom-transfer reaction with transition metal complex.

reaction of organic halides (R–X) with transition metals (M) proceeds via the redox mechanism involving a [R–X···M] complex as an intermediary species, and the formal oxidation state of the metal species is increased by one, and M–X is formed by the halogen abstraction.[9] In the [R–X···M] complex, M has to be coordinatively unsaturated, and thus, use of isolated coordinatively unsaturated complexes as the catalyst could facilitate the production of [R–X···M], which subsequently undergoes atom-transfer process to produce the radical species ($R^{\cdot}$) to initiate the reaction. If M has appropriate redox potentials, the catalytic cycle illustrated in Scheme 1 could be successfully operated.

In fact, ruthenium amidinate complexes **1**–**3** showed a coordinatively unsaturated nature, and actually behaved as efficient catalysts for ATRR as described in our previous papers.[6c,7] For further studies in this line, we were interested in isolable ruthenium alkoxides $[(\eta^5\text{-}C_5Me_5)Ru(OR)]_2$ **4**, which exist in solution as coordinatively unsaturated dimers having 32 valence electrons and reversibly forms monomers in contact with appropriate ligands.[10] The formed monomer, which was stabilized by the ligand, is still coordinatively unsaturated (16 valence electrons), being able to accept the coordination of R–X for its activation.[10c,11] In this paper, we wish to report that coordinatively unsaturated ruthenium alkoxides actually behave as the catalyst for the cyclization of *N*-allyl-α,α-dichloroacetamides **5** and related reactions. The scope of these ruthenium alkoxides as catalysts for ATRC is described in relation to the low-temperature activation of organic halides and stereochemical outcomes of the reactions, and their performance is compared with that for atom-transfer radical polymerization (ATRP) (Scheme 2).

## 2. Results and discussion

### 2.1. Atom-transfer radical cyclization

As we expected, $[Cp^*Ru(OMe)]_2$ **4a** was effective for the activation of a C–Cl bond at ambient temperature.

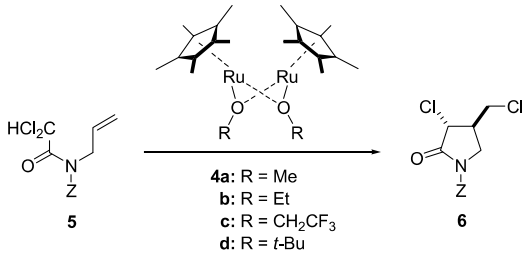


**Scheme 2.** ATRC of *N*-allyl-α,α-dichloroacetamides **5**.

Treatment of α,α-dichloroacetamide **5a** (0.2 mmol) with **4a** (10 mol% of Ru) in dichloromethane for 4 h under an argon atmosphere afforded the cyclic product **6a** in 50% isolated yield with a trans/cis ratio of 86:14 (Table 1, entry 1). The alkoxy group on the ruthenium apparently affected the catalytic activity; the ethoxy complex **4b** gave **6a** in 34% yield (entry 2), whereas no product was obtained by the use of trifluoroethyl and *t*-butyl derivatives (**4c** and **4d**) as catalysts (entries 3 and 4). It is noteworthy that ruthenium halide complexes such as $[Cp^*Ru^{II}Cl]_4$ and $[Cp^*Ru^{III}Cl_2]_2$ are not effective for this cyclization at ambient temperature (<5% yields). These results showed that the sterically less-hindered alkoxide ligand plays a crucial role in enhancing the reactivity of the ruthenium complexes towards organic halides via the one-electron redox process, which may be related to the π-donation by alkoxide lone pairs. Among the solvents examined, dichloromethane proved to be the most effective for both chemical yield and trans/cis ratio of the product (entries 5–8).

**Table 1**. Radical cyclization of **5a** with $[Cp^*Ru(OR)]_2$ **4a**–**d**[a]

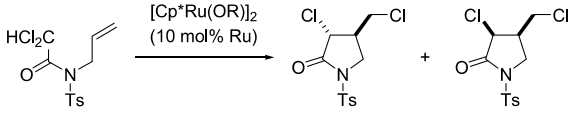


| Entry | Cat. | Solvent | Time (h) | Yield (%) | trans/cis[b] |
|---|---|---|---|---|---|
| 1 | **4a** | $CH_2Cl_2$ | 4 | 50 | 86:14 |
| 2 | **4b** | $CH_2Cl_2$ | 4 | 34 | 85:15 |
| 3 | **4c** | $CH_2Cl_2$ | 4 | 0 | — |
| 4 | **4d** | $CH_2Cl_2$ | 4 | 0 | — |
| 5 | **4a** | $CH_2Cl_2$ | 16 | 64 | 86:14 |
| 6 | **4a** | Benzene | 16 | 33 | 83:17 |
| 7 | **4a** | MeCN | 16 | 32 | 82:18 |
| 8[c] | **4a** | $Et_2O$ | 16 | <10 | 78:22 |

[a] All reactions were carried out using 0.2 mmol of **5a**, 0.01 mmol of **4** in 1.5 mL of solvent at room temperature.
[b] Determined by $^1$H NMR analysis.
[c] 0.03 mmol (30 mol% Ru) was used.

Despite the high catalytic activity for the cyclization of dichloroacetamide **5a**, a disadvantage of **4a** is its short lifetime as shown in the reaction profiles (Fig. 2, left; a); the reaction was terminated after some of the starting materials were consumed (~80%, TON≤8). Although the catalytic activity (initial reaction rate) was slightly decreased, addition of pyridine to the reaction mixture depresses inactivation of the catalyst (Fig. 2, left; b). The effects of pyridine and other ligands, which affect the catalytic efficiency in the reaction of **5a** with **4a** in dichloromethane at ambient temperature, are summarized in Table 2.

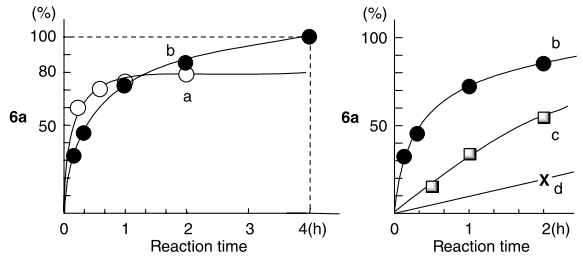


**Figure 2.** The plots of formed **6a** (%) versus time (h): (a) catalyzed by **4a** (○); (b) catalyzed by **4a**/pyridine (●); (c) catalyzed by **3** (□); (d) catalyzed by CuCl/bipyridine (×).

**Table 2**. Additive effects in the reaction of **5a** with **4a**[a]

| Entry | Additive | Additive/Ru | Yield (%) | Trans/cis[b] |
|---|---|---|---|---|
| 1 | — | — | 50 | 86:14 |
| 2 | $PPh_3$ | 0.5 | 95 | 87:13 |
| 3 | DMAP | 0.5 | 91 | 89:11 |
| 4 | Pyridine | 0.5 | >99 | 87:13 |
| 5 | Pyridine | 1.0 | >99 | 87:13 |
| 6 | Pyridine | 2.0 | >99 | 87:13 |
| 7 | Pyridine | 3.0 | 89 | 87:13 |
| 8 | Pyridine | 0.25 | >99 | 87:13 |

[a] All reactions were carried out using 0.2 mmol of **2**, 0.01 mmol of **4a** and additive in 1.5 mL of $CH_2Cl_2$ at room temperature for 4 h.
[b] Determined by $^1$H NMR analysis.

Remarkable improvement in the catalytic efficiency was achieved by the addition of donor ligands (0.5 equiv for Ru), and pyridine proved to be the most effective for this catalyst system (entries 1 vs 2–4). We also found that the addition of 0.25–2.0 equiv of pyridine for Ru resulted in satisfactory yields within 4 h (entries 4–8). It is noteworthy that both the catalytic activity and efficiency of the present $[Cp^*Ru(OMe)]_2$/pyridine system exceeds those of either the CuCl/bipyridine or the cationic diruthenium amidinate systems; the conventional Cu-catalyzed cyclization of dichloroacetamide is very slow at that temperature (2 h, 20% yield). The reaction catalyzed by the ruthenium complex **3**, which is the most effective catalyst for this type of cyclization, was faster than that with the CuCl/bypridine system but slower than that with **4a**, but terminated before reaching completion (3 h, 88% yield) (Fig. 2, right).

Table 3 summarizes the results obtained for the reaction of various *N*-allyl-α,α-dichloroacetamides **5a–e** catalyzed by 5 mol% of $[Cp^*Ru(OMe)]_2$ **4a** (i.e., 10 mol% Ru) and 5 mol% of pyridine (Ru/pyridine = 0.5) in dichloromethane (1.5 mL). In all reactions, the product was formed in high yields, except in the case of the N–H congener **5e** (entry 6). High catalytic activity of the present catalyst system was also demonstrated in the cyclization of *N*-benzyl and *N*-phenyl derivatives **5c** and **5d**, which are both known as less reactive substrates than **5a** and **5b**.[4f,12] Although the reaction of **5c** with this catalyst system was not so fast at room temperature (20 h; 76% yield), the reaction at 40 °C for 7 h gave the product **6c** in quantitative yield (entries 3 and 4). In the reaction of **5d**, the cyclic product **6d** was obtained in 90% isolated yield by the use of 30 mol% Ru at room temperature for 17 h (entry 5). In all cases, the trans/cis ratio of the product was controlled as ca. 4:1. The relative stereochemistry of the major isomer of **6d** was determined to be 3,4-*trans* by X-ray diffraction (Fig. 3, left). The 3,4-*trans* stereochemistry of major products **6a–c** was assigned by the similarity seen in the $^1$H NMR spectra to those reported by Slough[8a] and Gelfi.[8b]

**Table 3**. Radical cyclization of various *N*-allyldichloroacetamides **5a–d**[a]

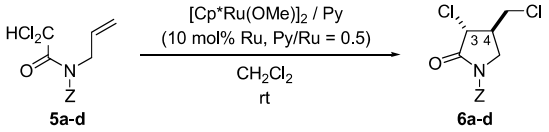


| Entry | Substrate | Time (h) | Yield (%) | Trans/cis[b] |
|---|---|---|---|---|
| 1 | **5a** (Z=Ts) | 4 | 92 | 87:13 |
| 2 | **5b** (Z=Allyl) | 5 | 95 | 80:20 |
| 3 | **5c** (Z=Bn) | 20 | 76 | 81:19 |
| 4[c] | **5c** | 7 | >99 | 82:18 |
| 5[d] | **5d** (Z=Ph) | 17 | 90 | 83:17 |
| 6 | **5e** (Z=H) | 4 | <1 | — |

[a] All reactions were carried out using 0.2 mmol of **5**, 0.01 mmol of **4a** and 0.01 mmol of pyridine in 1.5 mL of $CH_2Cl_2$ at room temperature.
[b] Determined by $^1$H NMR analysis.
[c] In dichloroethane at 40 °C.
[d] 0.03 mmol of **4a** (30 mol% Ru) and 0.03 mmol of pyridine were used.

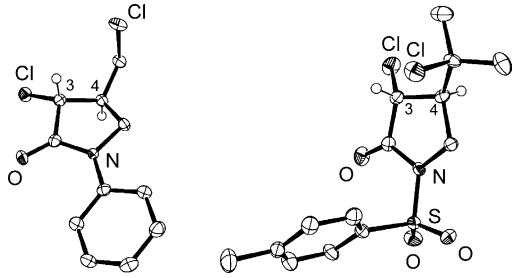


**Figure 3.** The ORTEP drawings of 3,4-*trans*-**6d** (left) and 3,4-*trans*-**10a** (right). For clarify, only H atoms at the C3 and C4 positions are shown.

The efficiency of $[Cp^*Ru(OMe)]_2$/pyridine system eventually led to three important aspects in the ATRC. First, the reaction of *N*-tosyl-α,α-dichloroacetamides **7a** and **7b** bearing substituted allyl groups such as prenyl and methallyl moieties, which are less reactive substrates than the *N*-allyl homologue **5a**,[8e] proceeded even at ambient temperature to afford the corresponding γ-lactams **10a** and **10b** in good yields (Table 4, entries 1 and 2). The relative stereochemistry of the major product **10a** was determined to be 3,4-*trans* by X-ray diffraction (Fig. 3, right). It is noteworthy that the diastereoselectivity of the reaction of methallyl derivative **7b** reaches to 93:7. The 3,4-*trans* configuration of the major product **10b** was determined by difference NOE experiments; no NOEs were obtained between the methine proton ($H^3$) at the 3-position and the methyl protons at the 4-position (4-Me) for the major isomer, whereas 6.7% NOE to 4-Me by irradiation of $H^3$ and 10.7% NOE to $H^3$ by irradiation of 4-Me for the minor isomer. This catalyst system was also effective for the cyclization of α-monobromoacetamide **8** and the corresponding brominated γ-lactam **11** was obtained in 98% yield (entry 3). Application of this catalyst system to β-lactam synthesis is also possible; 4-*exo* cyclization predominantly proceeded by the reaction of *N*-vinylacetamides **9a** and **9b** to give the corresponding β-lactams **12a** and **12b** in quantitative yields as the sole products (entries 4 and 5).

**Table 4**. Radical cyclization of various acetamides **9–11**[a]

| Entry | Substrate | Time (h) | Product (trans/cis)[b] | Yield (%) |
|---|---|---|---|---|
| 1[c] | 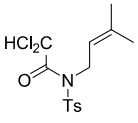 **7a** | 4 | 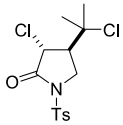 **10a** (80:20) | 80 |
| 2 | 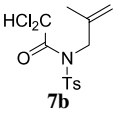 **7b** | 16 | 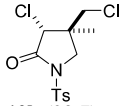 **10b** (93:7) | 70 |
| 3[d] | 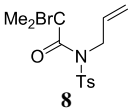 **8** | 4 | 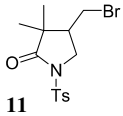 **11** | 98 |
| 4 | 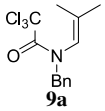 **9a** | 4 | 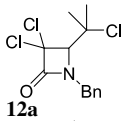 **12a** | >99 |
| 5 | 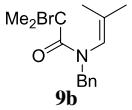 **9b** | 4 | 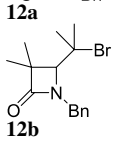 **12b** | >99 |

[a] All reactions were carried out using 0.02 mmol of substrate, 0.03 mmol of **4a** and 0.03 mmol of pyridine in 1.5 mL of $CH_2Cl_2$ at room temperature.
[b] Determined by $^1$H NMR analysis.
[c] 0.02 mmol of **4a** (20 mol% Ru) and 0.02 mmol of pyridine were used.
[d] 0.01 mmol of **4a** (10 mol% Ru) and 0.01 mmol of pyridine were used.

The advantage of the coordinatively unsaturated $[Cp^*Ru(OMe)]_2$ complex **4a** is its easy preparation by the literature method[10b–d] and the redox properties suitable for the ATRC of *N*-allyl dichloroacetamides. It is known that there are some relations between the redox properties and the efficiency of the catalyst in the conventional CuCl/bipyridine catalyst system and the coordinatively unsaturated diruthenium amidinate **3** active for ATRC.[7b] The redox potentials for CuCl/bipyridine in THF is $E_{pa}=+0.03$ V, $E_{pc}=-0.13$ V [$Cu^I/Cu^{II}$], whereas that of **3** is $E_{pa}=-0.002$ V, $E_{pc}=-0.05$ V [$Ru^{II}/Ru^{III}$]. In contrast, cyclic voltammogram of **4a** (R=Me) in THF shows a quasi-reversible one-electron oxidation wave ($E_{pa}=-0.13$ V, $E_{pc}=-0.20$ V versus $Ag/Ag^+$ at the scan rate of 0.1 V/s) due to the $Ru^{II}/Ru^{III}$ oxidation process. These data showed that the ruthenium methoxide **4a** is a stronger electron donor than the CuCl/bipyridine and the diruthenium amidinate **3**, and reasonably explain facile activation of a C–Cl bond in *N*-allyl dichloroacetamides, less reactive substrates than *N*-allyl trichloroacetamides.

An interesting feature of the **4a**-catalyzed cyclization of *N*-allyl dichloroacetamides is its stereoselectivity. It is known that equilibrium between the *trans*- and *cis*-isomers of the γ-lactams **6** formed from α,α-dichloroacetamides **5** took place easily in the presence of transition metal complexes over 80 °C.[13] For example, the thermodynamically controlled ratio of *trans*-**6a** to *cis*-**6a** reached ca. 4:1; this is in accord with that the ab initio study predicts energy difference between two isomers to be ca. 3 kcal/mol.[14] The diastereomer ratio of **6a** obtained by the present catalyst system is ca. 6.7:1, and no equilibrium between the two isomers is observed in the presence of the catalyst at room temperature. These results suggest that the reaction of α,α-dichloroacetamides **5** by the **4a**/pyridine catalyst is controlled kinetically, which is similar to the cationic diruthenium amidinate **3** reported previously.[7] Interestingly, MO calculations indicate that there is no substantial energy difference (<0.1 kcal/mol)[14] between *trans*-**10b** and *cis*-**10b** in the case of the reaction of **7b**. Furthermore, activation energies of both pathways via the free radical mechanism are almost the same (ca. 5 kcal/mol).[15] Nevertheless, higher trans-selectivity of the cyclization of **7b** (*N*-methallyl:trans/cis=ca. 13.3:1) was observed than that of **5a** (*N*-allyl:trans/cis=ca. 6.7:1). This may be explained by the Ru-coordinated transition states (Fig. 4). Both 3,4-*cis*-**6a** and 3,4-*cis*-**10b** are obtained via the transition states **A** and **B**. In the transition state **B**, the steric repulsion between the methyl substituent of **7b** and bulky $\eta^5$-$C_5Me_5$ ligand on the Ru is expected to be more important than that between H and $\eta^5$-$C_5Me_5$ ligand in **A**. Therefore, the cyclization of **7b** proceeds through the transition state **C**, which affords the 3,4-*trans* isomer.

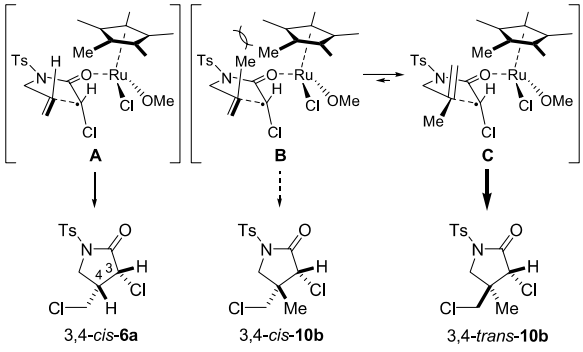


**Figure 4.** Proposed transition states.

It is well known that radical cyclization of ω-olefinic haloamides at low temperatures has a problem of low yields of the product due to high rotational barrier (16–22 kcal/mol) of the $C_{carbonyl}$–N.[4f,12] As shown in Scheme 3, there are two possible rotamers, *anti*-**5** and *syn*-**5**, and *anti*-**5** is the rotamer unfavorable for the cyclization. From the $^1$H NMR spectra of amides **5a** (Z=Ts) and **5d** (Z=Ph), single set of signals is observed. However, the spectrum of **5c** (Z=Bn) shows two sets of signals (ca. 1:1) due to the rotational isomers around the $C_{carbonyl}$–N bond. Preliminary DFT caluculations[14] suggest that there is no substantial energy difference between two rotamers of **5a**

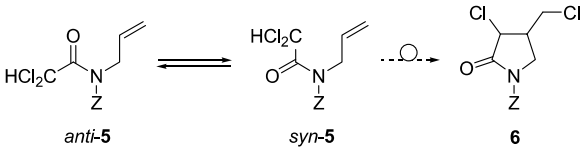


**5a:** *anti* ≈ *syn* (< 0.3 kcal/mol))
**5b:** *anti* = *syn*
**5c:** *anti* < *syn* (0.7 kcal/mol)
**5d:** *anti* > *syn* (4.3 kcal/mol)

**Scheme 3.** The conformation of **5a–d** in solution.

(<0.3 kcal/mol) and **5c** (0.7 kcal/mol), whereas *anti*-**5d** (4.3 kcal/mol) is the stable conformer for the other one. We have previously reported that the rotation barrier of the *N*-tosylated acetamides was much lower than that of the *N*-benzyl derivatives; *syn–anti* interconversion of the tosyl-protected amides was first in the NMR time scale, leading to the appearance of a single set of sharp signals.[4f,12d] Two apparent reasons of higher reactivity of **5a** than that of **5c** and **5d** are the introduction of the electron-withdrawing substituent on the N atom, which lowers the LUMO of the α-C–Cl bond described above, and facile formation of the rotamer favorable for the cyclization by the amide rotation. While in the case of **5c** and **5d**, high population of the undesired rotamer makes the reaction slower, but the reactivity of the catalyst is high enough to provide the product under milder conditions (<40 °C) than the cyclization catalyzed by the conventional CuCl/bipyridine catalyst. Such high reactivity may be explained by the oxophilic nature of the coordinatively unsaturated ruthenium methoxide, which could provide its interaction with the oxygen atom of amide **5**. As shown in Scheme 4, the coordination makes *syn*-**D** a more favorable conformation than *anti*-**D** because of the steric repulsion between the Cl atom at the α-position and the substituent (Z) on the N atom.

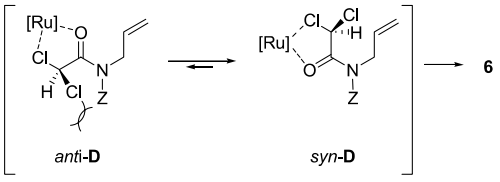


**Scheme 4.** The conformation of Cp*Ru(OMe)/**5** in the cyclization.

One of the most interesting questions in this cyclization is what is a net catalyst species in solution. As noted above, the ruthenium alkoxides **4** exist as a dimer in crystal structures,[10c,d] whereas they are possibly dissociated to the corresponding monomer in contact with appropriate ligand. In fact, the several coordinatively unsaturated Cp*Ru(OR)L were isolated and characterized by Caulton and coworkers.[10g] Since the addition of auxiliary ligands is important for efficient catalytic reactions, a probable answer is the reaction proceeding through a monomeric active species. Although clear evidence for the complexation between $[Cp^*Ru(OMe)]_2$ **4a** and pyridine was not visible on the $^1H$ NMR spectrum of a mixture of **4a** and pyridine, in which only dimeric **4a** and free pyridine were observed, we consider at present stage that the coordination can take place reversibly, and a small amount of active catalyst stabilized by pyridine promote the cyclization. In other words, the success of **4a**/pyridine system for the ATRC is provided by the stabilization of the coordinatively unsaturated, unstable monomeric Cp*Ru(OMe) species with pyridine (Scheme 5, **E**). The ATRC of **5** proceeds via the complex **E** to afford the product **6**. Then the stable dimer **4a** and free pyridine are regenerated, as shown in Scheme 5.

## 2.2. Atom-transfer radical polymerization

In the above sections, we have demonstrated high catalytic reactivity of the coordinatively unsaturated $[Cp^*Ru(OMe)]_2$

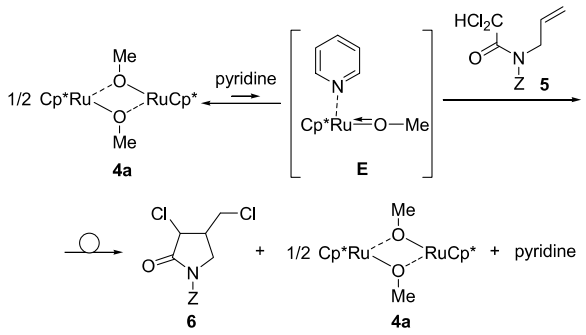


**Scheme 5.** Proposed reaction mechanisms for ATRC catalyzed by **4a**/pyridine system.

**4a** having appropriate redox potentials for ATRC in the presence of pyridine. The success of these studies prompted us to extend catalysis of the coordinatively unsaturated ruthenium methoxide to ATRP. As described in our previous paper,[7b] coordinatively unsaturated species facilitates the initial step of ATRC, cleavage of a C–X bond of the substrate, which is the most important point for the catalytic cycle as shown in Scheme 1. In contrast, the catalyst for ATRP has to play important roles not only for the activation of the organic halide initiators to start the polymerization but also the reactivation of a C–X bond at the terminal of the intermediate polymer (the dormant species) as shown in Scheme 6. The coordinatively unsaturated species should be advantageous to take part in the facile activation of the organic halide initiators and the dormant species. In contrast, a possible drawback deduced from our results of ATRC is instability of the coordinatively unsaturated species, which makes the reactivation of dormant species ineffective in the time running. The deactivation of the catalyst should affect the polymerization behavior. Sawamoto and coworker reported a coordinatively unsaturated ruthenium complex, $Ru(Cp^*)Cl(PCy_3)$, catalyzes rapid but 'ill-controlled' polymerization of methyl methacrylate (MMA) to give poly(MMA) with quite broad molecular weight distributions ($M_w/M_n=2.8$–$6.2$).[16] In sharp contrast, we found that the coordinatively unsaturated ruthenium amidinate **3** can effectively activate a C–X bond of organic halides resulting in the formation of poly(MMA) having a halogen atom end group with narrow molecular weight distributions ($M_w/M_n \leq 1.3$), but the polymerization is terminated before complete conversion of monomers.[7b]

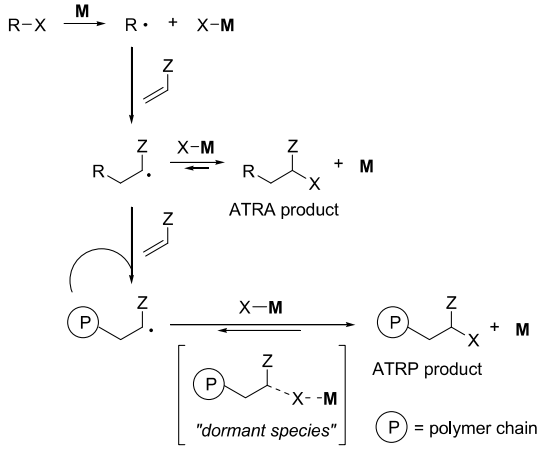


**Scheme 6.** Proposed mechanisms for ATRP.

**Table 5**. Radical polymerization of MMA with **4a**[a]

| Entry | Initiator | Additive[b] | Yield (%)[c] | $M_n$[d] | $M_w/M_n$[d] |
|---|---|---|---|---|---|
| 1 | $CCl_4$ | — | 16 | 3900 | 1.3 |
| 2 | $CCl_4$ | Pyridine | 20 | 3100 | 1.2 |
| 3 | $Cl_3CCO_2Me$ | — | 21 | 5500 | 1.4 |
| 4 | $Cl_3CCO_2Me$ | Pyridine | 20 | 4000 | 1.2 |
| 5 | $Cl_2HCCO_2Et$ | — | 17 | 9600 | 1.6 |
| 6 | $Cl_2HCCO_2Et$ | Pyridine | 18 | 7000 | 1.3 |

[a] All reactions were carried out using 9.5 μmol of **4a**, 9.5 mmol of MMA, and 38 μmol of initiator in 2 mL of ethyl acetate at 60 °C for 12 h.
[b] 0.5 equiv for Ru was used.
[c] Determined by $^1$H NMR analysis.
[d] Determined by GPC analysis of the crude product.

A mixture of $[Cp^*Ru(OMe)]_2$ **4a** (9.5 μmol), MMA (1 mL, 9.5 mmol), and initiator (38 μmol) was stirred at 60 °C for 12 h (Table 5). The reaction using carbon tetrachloride as an initiator produced poly(MMA) with $M_n=3900$; $M_w/M_n=1.3$ in 16% yield as shown in entry 1. The molecular weight distribution of formed polymer was slightly improved ($M_w/M_n=1.2$) by the addition of pyridine (0.5 equiv for Ru), but the averaged molecular weight ($M_n$) decreased (entries 1 vs 2). The polymerization was also achieved by the use of α,α,α-trichloro- and α,α-dichloroacetates as initiators (entries 3–6). In all cases, the present polymerization was terminated within 3 h, showing that **4a** is reactive; but has a short lifetime.[17]

We also examined the activation of a carbon–halogen bond of macroinitiators, which is known to be less reactive than that of commonly used organic initiators. Matyjaszewski reported the polymerization of MMA with CuBr/dNbipy [dNbipy=4,4′-di(5-nonyl)-2,2′-bipyridine] using poly(THF)-derived bromopropionate as the initiator, in which a temperature over 90 °C (24 h, >97% conversion) was required for the reaction.[18a] The ruthenium methoxide **4a** catalyzed the polymerization of MMA using the macroinitiator **13**[18,19] derived from polybutylene oxides, [poly(THF)], bearing a 2-bromoisobutyl group at the polymer terminal ($M_n=3800$; $M_w/M_n=1.2$)[7b] at 25 °C for 4 h to form the polymer of $M_n=35{,}000$ and $M_w/M_n=1.4$; the $^1$H NMR spectrum of the obtained copolymer revealed that the product contains both poly(THF) and poly(MMA) segments (Scheme 7).[20] In the conversion of this particular polymerization, the chain growth was terminated after 47% of MMA was consumed (42% isolated yield). These results clearly showed that **4a** acts as an efficient catalyst for the activation of a C–Br bond of less reactive macromolecule initiator at low temperature, but the catalyst system is not stable enough to achieve the complete conversion of the monomers.

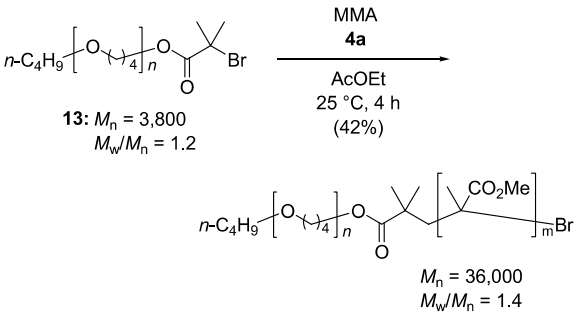


**Scheme 7.** Polymerization of MMA using macroinitiator **13**.

## 3. Conclusion

In our examinations for the coordinatively unsaturated ruthenium alkoxide, $[(\eta^5\text{-}C_5Me_5)Ru(OMe)]_2$ **4a**, as the ATRC and ATRP catalyst, we found that **4a** can effectively activate a C–X bond of organic or macromolecular halides at low temperature (room temperature).[21] In the cyclization reaction, the **4a**/pyridine system is useful for the synthesis of both β- and γ-lactams under mild conditions. The catalytic activity of the present system is even higher than the conventional CuCl/bipyridine catalyst and the diruthenium amidinate complex **3**. This clearly shows an advantage of coordinatively unsaturated complexes in catalyst efficiency for the halogen abstraction at the initial stage of the catalytic cycle, which especially contributes to rapid ATRC and controlling the relative stereochemistry of newly formed stereocenters. This catalyst system is also active towards polymerization of methacrylate using poly(THF)-derived macroinitiator, giving poly(THF)–poly(MMA) block copolymer with narrow molecular weight distributions; however, the polymerization is often accompanied by the catalyst deactivation leading to low conversion of the monomer. In other words, the present coordinatively unsaturated polymerization catalyst has a strong point in the efficiency but not in the durability. Consequently, the results presented in this paper demonstrate that the use of coordinatively unsaturated species is a reasonable strategy for the development of good catalysts for ATRC. For their application to ATRP, the polymerization is well-controlled at the initial stage, however, durability has somehow to be added to the catalyst to achieve high conversion of the monomer. These findings provide important aspects in catalyst search for atom-transfer radical reactions.

## 4. Experimental

### 4.1. General methods

All reactions were carried out under a nitrogen or argon atmosphere. Solvents were distilled under an inert gas atmosphere from $CaH_2$ (dichloromethane, acetonitrile and dichloroethane) or sodium/benzophenone (benzene and ether) prior to use. Carbon tetrachloride was purchased from Wako Pure Chemical Ind., Ltd. Methyl trichloroacetate and ethyl dichloroacetate were purchased from Tokyo Chemical Industry Co., Ltd. $^1$H and $^{13}$C NMR spectra were measured on JEOL ECA 400 (400 MHz) and ECA 600 (600 MHz) spectrometers. Chemical shifts for $^1$H NMR are described in parts per million downfield from tetramethylsilane as an internal standard ($\delta=0$) in $CDCl_3$, unless otherwise noted. Chemical shifts for $^{13}$C NMR are expressed in parts per million in $CDCl_3$ as an internal standard ($\delta=77.1$), unless otherwise noted. IR spectra were measured on a JASCO FT/IR-550 spectrometer. Column chromatography was performed with silica gel (Merck, Art 7734). Elemental analysis was performed by the Elemental Analysis Center, Faculty of Science, Kyushu University. HRMS analysis was performed by the Analytical Center in Institute for Materials Chemistry

and Engineering, Kyushu University. Analytical thin-layer chromatography (TLC) was performed on glass plates and aluminum sheets precoated with silica gel (Merck, Kieselgel 60 $F_{254}$, layer thickness 0.25 and 0.2 mm, respectively). Visualization was accomplished by UV light (254 nm), anisaldehyde, and phosphomolybdic acid. GPC analyses of the polymers were performed with a JASCO DG-1580-83 degasser, PU-980 HPLC pump, UV-970 UV/vis detector, RI-930 RI detector, and CO-2065-plus column oven (at 40 °C) using a Shodex GPC-KF-804L connected with a GPC KF-805L in THF. Calibration was carried out on the basis of retention time of a standard sample of poly(methyl methacrylate) (Shodex Standard M-75) 7 samples ($M_w/M_n$=1.02–1.09), of which the $M_n$ range is $1.84\times10^3$–$1.99\times10^6$. [($\eta^5$-$C_5Me_5$)Ru(OR)]$_2$ complexes **4a–d**[10b–d] were prepared by the literature methods. Acetamide derivatives **5**, **7–9** were prepared according to the literature methods.[4,8] Macroinitiator **13** was prepared by our method.[7b,19a]

### 4.2. General procedure for the atom-transfer radical cyclization of *N*-allyl-α-halogenated acetamies catalyzed by [($\eta^5$-$C_5Me_5$)Ru(OMe)]$_2$/bipyridine system

In a typical example, [($\eta^5$-$C_5Me_5$)Ru(OMe)]$_2$ (**4a**, 5.3 mg, 0.01 mmol, 10 mol% Ru) was measured into a flask, then freshly distilled, carefully degassed dichloromethane (1.5 mL) and pyridine (0.8 μL, 0.5 equiv for Ru) were added. This catalyst solution was transferred to the reaction flask in which contains *N*-allyl-*N*-tosyl-2,2-dichloroacetamide (**5a**, 64.4 mg, 0.2 mmol). After the resulting solution was stirred at ambient temperature for 4 h, the reaction mixture was filtered through a pad of Celite and Florisil, and then the filtrate was concentrated under reduced pressure. Purification by silica gel chromatography (1:1 hexane/ether) gave the product (**6a**) in 92% yield (59.3 mg): the cis/trans ratio was determined by $^1$H NMR analysis.

**4.2.1. 3-Chloro-4-chloromethyl-1-(*p*-toluenesulfonyl)-pyrrolidin-2-one (6a).**[8a] *trans-Isomer*. $^1$H NMR (600 MHz, $CDCl_3$): $\delta$=2.46 (s, 3H), 2.82 (m, 1H), 3.68–3.78 (m, 3H), 4.11 (dd, $J$=10.2, 8.1 Hz, 1H), 4.34 (d, $J$=9.3 Hz, 1H), 7.34 (d, $J$=8.3 Hz, 2H), 7.94 (d, $J$=8.3 Hz, 2H); $^{13}$C NMR (150 MHz, $CDCl_3$): $\delta$=21.8, 42.3, 44.2, 47.0, 56.1, 128.3, 130.0, 134.3, 146.1, 166.7.

*cis-Isomer*. $^1$H NMR (600 MHz, $CDCl_3$): $\delta$=2.46 (s, 3H), 2.95 (ddddd, $J$=8.3, 7.6, 7.3, 6.8, 6.1 Hz, 1H), 3.53 (dd, $J$=11.5, 7.6 Hz, 1H), 3.66 (dd, $J$=10.3, 8.3 Hz, 1H), 3.71 (dd, $J$=11.5, 6.8 Hz, 1H), 4.13 (dd, $J$=10.3, 7.3 Hz, 1H), 4.44 (d, $J$=6.1 Hz, 1H), 7.37 (d, $J$=8.3 Hz, 2H), 7.92 (d, $J$=8.3 Hz, 2H); $^{13}$C NMR (150 MHz, $CDCl_3$): $\delta$=21.8, 40.4, 41.0, 47.9, 57.6, 128.2, 130.0, 134.0, 146.0, 166.8.

**4.2.2. 3-Chloro-4-chloromethyl-1-allyl-pyrrolidin-2-one (6b).** IR (neat): $\nu$=1705 cm$^{-1}$; HRMS. Calcd for $C_8H_{11}Cl_2NO$: [M]=207.0218. Found: [M]=207.0211; *trans-Isomer*. $^1$H NMR (600 MHz, $CDCl_3$): $\delta$=2.87 (ttd, $J$=8.2, 6.6, 4.4 Hz, 1H), 3.28 (dd, $J$=9.9, 6.6 Hz, 1H), 3.53 (dd, $J$=9.9, 8.2 Hz, 1H), 3.72 (dd, $J$=11.5, 6.6 Hz, 1H), 3.76 (dd, $J$=11.5, 4.4 Hz, 1H), 3.91 (dd, $J$=14.8, 6.0 Hz, 1H), 3.97 (dd, $J$=14.8, 6.0 Hz, 1H), 4.37 (d, $J$=8.2 Hz, 1H), 5.24 (d, $J$=17.0 Hz, 1H), 5.26 (d, $J$=10.4 Hz, 1H), 5.72 (ddt, $J$=17.0, 10.4, 6.0 Hz, 1H); $^{13}$C NMR (150 MHz, $CDCl_3$): $\delta$=43.5, 44.8, 45.9, 47.0, 56.6, 119.2, 131.1, 168.3.

*cis-Isomer*. $^1$H NMR (600 MHz, $CDCl_3$): $\delta$=2.92 (tdt, $J$=8.2, 7.1, 6.6 Hz, 1H), 3.28 (dd, $J$=9.9, 8.2 Hz, 1H), 3.47 (dd, $J$=9.9, 7.1 Hz, 1H), 3.62 (dd, $J$=11.0, 8.2 Hz, 1H), 3.80 (dd, $J$=11.0, 6.6 Hz, 1H), 3.88–4.00 (m, 2H), 4.46 (d, $J$=6.0 Hz, 1H), 5.20–5.27 (m, 2H), 5.72 (m, 1H); $^{13}$C NMR (150 MHz, $CDCl_3$): $\delta$=40.7, 42.0, 45.5, 48.1, 57.6, 118.9, 131.1, 169.0.

**4.2.3. 3-Chloro-4-chloromethyl-1-benzyl-pyrrolidin-2-one (6c).**[4e,8b] Diastereomer ratio was determined by capillary GLC analysis: TC-17 (30 M), column temperature 240 °C, ditection FID, $t_R$=20.3 min (trans), 21.2 min (cis). *trans-Isomer*. $^1$H NMR (400 MHz, $CDCl_3$): $\delta$=2.82 (ddddd, $J$=9.0, 8.1, 7.1, 6.1, 4.9 Hz, 1H), 3.17 (dd, $J$=10.0, 7.1 Hz, 1H), 3.43 (dd, $J$=10.0, 8.1 Hz, 1H), 3.66 (dd, $J$=11.7, 6.1 Hz, 1H), 3.70 (dd, $J$=11.7, 4.9 Hz, 1H), 4.40 (d, $J$=9.0 Hz, 1H), 4.43 (d, $J$=14.6 Hz, 1H), 4.58 (d, $J$=14.6 Hz, 1H), 7.19–7.41 (m, 5H); $^{13}$C NMR (100 MHz, $CDCl_3$): $\delta$=43.5, 44.9, 47.0, 47.5, 56.8, 128.2, 128.3, 129.0, 135.2, 168.6.

*cis-Isomer*. $^1$H NMR (400 MHz, $CDCl_3$): $\delta$=2.87 (ddddd, $J$=8.1, 7.8, 7.1, 6.8, 6.3 Hz, 1H), 3.16 (dd, $J$=10.0, 8.1 Hz, 1H), 3.36 (dd, $J$=10.0, 7.1 Hz, 1H), 3.57 (dd, $J$=11.2, 7.8 Hz, 1H), 3.77 (dd, $J$=11.2, 6.8 Hz, 1H), 4.43 (d, $J$=14.6 Hz, 1H), 4.51 (d, $J$=6.3 Hz, 1H), 4.57 (d, $J$=14.6 Hz, 1H), 7.19–7.41 (m, 5H); $^{13}$C NMR (100 MHz, $CDCl_3$): $\delta$=40.8, 42.0, 47.1, 48.0, 57.7, 128.1, 128.2, 129.0, 135.3, 169.4.

**4.2.4. 3-Chloro-4-chloromethyl-1-phenyl-pyrrolidin-2-one (6d).** *trans-Isomer*. White solid; mp 113–114 °C; elemental Anal. Calcd (%) for $C_{11}H_{11}Cl_2NO$: C, 54.12; H, 4.54; N, 5.74. Found: C, 53.79; H, 4.57; N, 5.70; $^1$H NMR (600 MHz, $CDCl_3$): $\delta$=2.99 (ddddd, $J$=8.8, 8.2, 7.7, 6.6, 3.8 Hz, 1H), 3.82 (dd, $J$=11.5, 6.6 Hz, 1H), 3.83 (dd, $J$=9.9, 7.7 Hz, 1H), 3.87 (dd, $J$=11.5, 3.8 Hz, 1H), 4.00 (dd, $J$=9.9, 8.2 Hz, 1H), 4.54 (d, $J$=8.8 Hz, 1H), 7.22 (t, $J$=7.1 Hz, 1H), 7.41 (dd, $J$=8.2, 7.1 Hz, 2H), 7.63 (d, $J$=8.2 Hz, 2H); $^{13}$C NMR (150 MHz, $CDCl_3$): $\delta$=43.1, 44.4, 48.6, 57.4, 120.0, 125.6, 129.1, 138.4, 167.4.

*cis-Isomer*. $^1$H NMR (600 MHz, $CDCl_3$): $\delta$=3.08 (m, 1H), 3.73 (dd, $J$=11.5, 8.2 Hz, 1H), 3.80–3.91 (m, 3H), 4.63 (d, $J$=6.0 Hz, 1H), 7.22 (m, 1H), 7.41 (m, 2H), 7.63 (m, 2H); $^{13}$C NMR (150 MHz, $CDCl_3$): $\delta$=40.3, 41.9, 49.8, 58.7, 120.2, 125.7, 129.1, 138.4, 167.4.

**4.2.5. 3-Chloro-4-chloroisopropyl-1-(*p*-toluenesulfonyl)-pyrrolidin-2-one (10a).** *trans-Isomer*. Elemental Anal. Calcd (%) for $C_{14}H_{17}Cl_2NO_3S$: C, 48.01; H, 4.89; N, 4.00. Found: C, 47.96; H, 4.90; N, 4.00; $^1$H NMR (600 MHz, $CDCl_3$): $\delta$=1.60 (s, 3H), 1.72 (s, 3H), 2.45 (s, 3H), 2.67 (ddd, $J$=8.8, 8.2, 7.7 Hz, 1H), 3.85 (dd, $J$=10.4, 7.7 Hz, 1H), 4.10 (dd, $J$=10.4, 8.8 Hz, 1H), 4.51 (d, $J$=8.2 Hz, 1H), 7.36 (d, $J$=8.8 Hz, 2H), 7.95 (d, $J$=8.8 Hz, 2H); $^{13}$C NMR (150 MHz, $CDCl_3$): $\delta$=21.7, 31.1, 31.4, 46.4, 52.9, 56.0, 69.6, 128.4, 129.9, 134.2, 146.0, 167.2.

*cis-Isomer*. $^1$H NMR (600 MHz, $CDCl_3$): $\delta$=1.53 (s, 3H), 1.62 (s, 3H), 2.42 (s, 3H), 2.91 (ddd, $J$=9.9, 6.6, 5.0 Hz,

1H), 3.92 (dd, $J$=10.4, 9.9 Hz, 1H), 4.20 (dd, $J$=10.4, 6.6 Hz, 1H), 4.34 (d, $J$=5.0 Hz, 1H), 7.30 (d, $J$=8.7 Hz, 2H), 7.74 (d, $J$=8.7 Hz, 2H); $^{13}$C NMR (150 MHz, $CDCl_3$): $\delta$=25.5, 30.6, 31.7, 41.0, 50.1, 57.0, 67.0, 127.1, 128.1, 134.0, 143.3, 166.7.

**4.2.6. 3-Chloro-4-chloromethyl-4-methyl-1-(*p*-toluenesulfonyl)-pyrrolidin-2-one (10b).** Elemental Anal. Calcd (%) for $C_{13}H_{15}Cl_2NO_3S$: C, 46.44; H, 4.50; N, 4.17. Found: C, 46.69; H, 4.58; N, 4.13. *Major isomer*. $^1$H NMR (600 MHz, $CDCl_3$): $\delta$=1.13 (s, 3H), 2.46 (s, 3H), 3.52 (d, $J$=11.5 Hz, 1H), 3.56 (d, $J$=11.5 Hz, 1H), 3.72 (d, $J$=10.4 Hz, 1H), 3.88 (d, $J$=10.4 Hz, 1H), 4.52 (s, 1H), 7.36 (d, $J$=8.8 Hz, 2H), 7.93 (d, $J$=8.8 Hz, 1H); $^{13}$C NMR (150 MHz, $CDCl_3$): $\delta$=18.5, 21.7, 43.9, 47.7, 52.8, 61.0, 128.1, 129.92, 134.2, 145.91, 166.4.

*Minor isomer*. $^1$H NMR (600 MHz, $CDCl_3$): $\delta$=1.31 (s, 3H), 2.46 (s, 3H), 3.37 (d, $J$=11.5 Hz, 1H), 3.54 (d, $J$=11.5 Hz, 1H), 3.63 (d, $J$=10.4 Hz, 1H), 4.00 (d, $J$=10.4 Hz, 1H), 4.18 (s, 1H), 7.36 (d, $J$=8.8 Hz, 2H), 7.93 (d, $J$=8.8 Hz, 1H); $^{13}$C NMR (150 MHz, $CDCl_3$): $\delta$=20.7, 21.7, 42.9, 47.3, 53.2, 63.3, 128.1, 129.86, 134.1, 145.89, 166.6.

**4.2.7. 3,3-Dimethyl-4-bromomethyl-1-(*p*-toluenesulfonyl)-pyrrolidin-2-one (11).**[8c] $^1$H NMR (600 MHz, $CDCl_3$): $\delta$=0.89 (s, 3H), 1.16 (s, 3H), 2.44 (s, 3H), 2.45 (dddd, $J$=9.9, 8.8, 7.7, 4.4 Hz, 1H), 3.20 (t, $J$=9.9 Hz, 1H), 3.43 (dd, $J$=9.9, 4.4 Hz, 1H), 3.46 (dd, $J$=10.4, 8.8 Hz, 1H), 4.15 (dd, $J$=10.4, 7.7 Hz, 1H), 7.34 (d, $J$=8.2 Hz, 2H), 7.91 (d, $J$=8.2 Hz, 2H); $^{13}$C NMR (150 MHz, $CDCl_3$): $\delta$=17.8, 21.7, 23.4, 29.7, 45.0, 45.4, 48.8, 128.0, 129.7, 134.8, 145.3, 176.8.

**4.2.8. 3,3-Dichloro-4-(1-chloroisopropyl)-1-benzyl-azetidin-2-one (12a).**[23] $^1$H NMR (600 MHz, $CDCl_3$): $\delta$=1.74 (s, 3H), 1.81 (s, 3H), 4.23 (s, 1H), 4.33 (d, $J$=14.9 Hz, 1H), 4.98 (d, $J$=14.9 Hz, 1H), 7.20–7.43 (m, 5H); $^{13}$C NMR (150 MHz, $CDCl_3$): $\delta$=26.2, 29.0, 46.2, 68.5, 77.8, 81.2, 128.3, 128.5, 128.9, 133.9, 161.7.

**4.2.9. 3,3-Dimethyl-4-(1-bromoisopropyl)-1-benzyl-azetidin-2-one (12b).**[24] $^1$H NMR (600 MHz, $CDCl_3$): $\delta$=1.27 (s, 3H), 1.39 (s, 3H), 1.80 (s, 3H), 1.81 (s, 3H), 3.60 (s, 1H), 4.23 (d, $J$=15.4 Hz, 1H), 4.92 (d, $J$=15.4 Hz, 1H), 7.27–7.36 (m, 5H); $^{13}$C NMR (150 MHz, $CDCl_3$): $\delta$=17.9, 24.0, 31.3, 32.6, 45.0, 55.3, 65.1, 72.8, 127.6, 128.5, 128.6, 136.1, 174.7. HRMS. Calcd for $C_{15}H_{20}BrNO$: [M]=309.0728. Found: [M]=309.0725.

### 4.3. Polymerization of MMA using macroinitiator 13

A mixture of $[Cp^*Ru(OMe)]_2$ **4a** (5 mg, 9 μmol), MMA (1 mL, 9.5 mmol), and macroinitiator **13** [$M_n$=3800, $M_w/M_n$=1.2] (68 mg, 18 μmol) was placed in a glass tube. The mixture was degassed three times, and sealed in vacuo. After it was stirred at 25 °C for 4 h, the reaction mixture was concentrated under reduced pressure. The residue was dissolved in THF and was purified by precipitation by adding methanol gave the block copolymer in 42% yield. The GPC analysis showed $M_n$=36,000, $M_w/M_n$=1.4.

### 4.4. Electrochemical measurements

Cyclic voltammetric studies were carried out using a BAS 50B/W electrochemical analyzer in a globe box filled with purified nitrogen. The measurement was performed at room temperature using a ruthenium or copper complex (0.0015 mmol) in THF (5 mL) containing $Bu_4NPF_6$ (0.1 M) as a supporting electrolyte. A three-electrode cell was used, which was equipped with a platinum disk working electrode, a platinum wire counter electrode, and a silver reference electrode comprised of a silver wire in count with $AgNO_3$ (0.01 M) and $Bu_4NPF_6$ (0.2 M) in acetonitrile.

### 4.5. X-ray structure determination and details of refinement

X-ray-quality crystals of **5a**, **6d** and **10a** were grown from a mixture of $CH_2Cl_2$ and hexane, and mounted in a glass capillary. All measurements were made on a Rigaku RAXIS RAPID imaging plate area detector with graphite monochromated Cu K$\alpha$ radiation; $\lambda$=1.54187 Å for **5a**, and on a Rigaku Saturn CCD area detector with graphite monochromated Mo K$\alpha$ radiation; $\lambda$=0.71070 Å. The crystal-to-detector distance was 127.40 mm for **5a**, 45.09 mm for **6d**, and 45.07 mm for **10a**. The data were collected at 123(1) K to a maximum 2$\theta$ value of 136.5° for **5a**, and of 55.0° for **6d** and **10a**. The structures were solved by direct methods,[25] and expanded using Fourier techniques.[26] The non-hydrogen atoms were refined anisotropically. Hydrogen atoms were refined using the riding model. The final cycle of full-matrix least-squares refinement on $F^2$ was based on 2393 observed reflections and 185 variable parameters for **5a**, on 2502 observed reflections and 148 variable parameters for **6d**, and on 3461 observed reflections and 207 variable parameters for **10a**. Neutral atom scattering factors were taken from Cromer and Waber.[27] All calculations were performed using the CrystalStructure[28,29] crystallographic software package. The numbering schemes employed are shown in Figure 3 (3,4-*trans*-**6a** and 3,4-*trans*-**10a**) and Supporting information (**5a**), which were drawn with ORTEP at 50% probability elipsoids. Crystallographic data (excluding structure factors) for the structure has been deposited with the Cambridge Crystallographic Data Centre as supplementary publication no. CCDC-290147 for **5a**, CCDC-290148 for 3,4-*trans*-**6d**, and CCDC-290149 for 3,4-*trans*-**10a**. Copies of the data can be obtained free of charge on application to CCDC, 12 Union Road, Cambridge CB21EZ, UK (fax: +44 1223 336 033; e-mail: deposit@ccdc.cam.ac.uk).

### Acknowledgements

We are grateful to Mr. Taisuke Matsumoto and Ms. Keiko Ideta (Analytical Center in Institute for Materials Chemistry and Engineering, Kyushu University) for their help in the X-ray and NOE analyses. This work was supported by a Grant-in-Aid for Scientific Research from the Ministry of Education, Culture, Sports, Science and Technology, Japan.

## Supplementary data

Supplementary data associated with this article can be found, in the online version, at doi:10.1016/j.tet.2006.01.011. Tables of crystal structure parameters and details of data correction, bond angles and distances, and atomic positional and thermal parameters of **5a**, 3,4-*trans*-**6d** and 3,4-*trans*-**10a**.

## References and notes


1. (a) Giese, B. *Radicals in Organic Synthesis: Formation of Carbon–Carbon Bonds*; Pergamon: New York, 1986. (b) Curran, D. P. In Trost, B. M., Fleming, I., Eds.; Comprehensive Organic Synthesis; Pergamon: Oxford, 1991; Vol. 4, p 715. (c) *Radicals in Organic Synthesis*; Renaud, P., Sibi, M. P., Eds.; Wiley-VCH: Weinheim, 2001.
2. (a) Kato, M.; Kamigaito, M.; Sawamoto, M.; Higashimura, T. *Macromolecules* **1995**, *28*, 1721. (b) Wang, J. S.; Matyjaszewski, K. *J. Am. Chem. Soc.* **1995**, *117*, 5614. (c) Patten, T. E.; Xia, T.; Abernathy, K.; Matyjaszewski, K. *Science* **1996**, *272*, 866.
3. Reviews: (a) *Controlled Radical Polymerization*; Matyjaszewski, K., Ed.; ACS Symposium Series 685; American Chemical Society: Washington, 1998. (b) Patten, T. E.; Matyjaszewski, K. *Adv. Mater.* **1998**, *10*, 901. (c) Sawamoto, M.; Kamigaito, M. In *Synthesis of Polymers*; Schlüter, A.-D., Ed.; Materials Science and Technology Series; Wiley-VCH: Weinheim, 1999; Chapter 6. (d) Matyjaszewski, K.; Xia, J. *Chem. Rev.* **2001**, *101*, 2921. (e) Kamigaito, M.; Ando, T.; Sawamoto, M. *Chem. Rev.* **2001**, *101*, 3689.
4. (a) Nagashima, H.; Wakamatsu, H.; Ito, K.; Tomo, Y.; Tsuji, J. *Tetrahedron Lett.* **1983**, *24*, 2395. (b) Nagashima, H.; Wakamatsu, H.; Itoh, K. *J. Chem. Soc., Chem. Commun.* **1984**, 652. (c) Nagashima, H.; Ozaki, N.; Seki, K.; Ishii, M.; Itoh, K. *J. Org. Chem.* **1989**, *54*, 4497. (d) Nagashima, H.; Seki, K.; Ozaki, N.; Wakamatsu, H.; Itoh, K.; Tomo, Y.; Tsuji, J. *J. Org. Chem.* **1990**, *55*, 985. (e) Nagashima, H.; Ozaki, N.; Ishii, M.; Seki, K.; Washiyama, M.; Itoh, K. *J. Org. Chem.* **1993**, *58*, 464. (f) Iwamatsu, S.; Matsubara, K.; Nagashima, H. *J. Org. Chem.* **1999**, *64*, 9625.
5. . Reviews: (a) Iqbal, J.; Bhatia, B.; Nayyar, N. K. *Chem. Rev.* **1994**, *94*, 519. (b) Giese, B.; Kopping, B.; Gobel, T.; Dickhaut, J.; Thoma, G.; Kulicke, K. J.; Trach, F. *Org. React.* **1996**, *48*, 301. (c) Clark, A. J. *Chem. Soc. Rev.* **2002**, *31*, 1.
6. (a) Yamaguchi, Y.; Nagashima, H. *Organometallics* **2000**, *19*, 725. (b) Kondo, H.; Kageyama, A.; Yamaguchi, Y.; Haga, M.; Kirchner, K.; Nagashima, H. *Bull. Chem. Soc. Jpn.* **2001**, *74*, 1927. (c) Nagashima, H.; Gondo, M.; Masuda, S.; Kondo, H.; Yamaguchi, Y.; Matsubara, K. *Chem. Commun.* **2003**, 442. Also see: (d) Nagashima, H.; Kondo, H.; Hayashida, T.; Yamaguchi, Y.; Gondo, M.; Masuda, S.; Miyazaki, K.; Matsubara, K.; Kirchner, K. *Coord. Chem. Rev.* **2003**, *245*, 177.
7. (a) Motoyama, Y.; Gondo, M.; Masuda, S.; Iwashita, Y.; Nagashima, H. *Chem. Lett.* **2004**, *33*, 442. (b) Motoyama, Y.; Hanada, S.; Niibayashi, S.; Shimamoto, K.; Takaoka, N.; Nagashima, H. *Tetrahedron* **2005**, *61*, 10216.
8. (a) Rachita, M. A.; Slough, G. A. *Tetrahedron Lett.* **1993**, *34*, 6821. (b) Benedetti, M.; Forti, L.; Ghelfi, F.; Pagnoni, U. M.; Ronzoni, R. *Tetrahedron* **1997**, *53*, 14031. (c) Clark, A. J.; Duncalf, D. J.; Filik, R. P.; Haddleton, D. M.; Thomas, G. H.; Wongtap, H. *Tetrahedron Lett.* **1999**, *40*, 3807. (d) Clark, A. J.; Filik, R. P.; Thomas, G. H. *Tetrahedron Lett.* **1999**, *40*, 4885. (e) Clark, A. J.; Filik, R. P.; Haddleton, D. M.; Radigue, A.; Sanders, C. J.; Thomas, G. H.; Smith, M. E. *J. Org. Chem.* **1999**, *64*, 8954.
9. (a) Minisci, F. *Acc. Chem. Res.* **1975**, *8*, 165. (b) Kochi, J. K. *Organometallic Mechanisms and Catalysis*; Academic: New York, 1978. (c) Davis, R.; Groves, I. F. *J. Chem. Soc., Dalton Trans.* **1982**, 2281.
10. Review: (a) Koelle, U. *Chem. Rev.* **1998**, *98*, 1313. Also see; (b) Koelle, U.; Kossakowski, J. *J. Chem. Soc., Chem. Commun.* **1988**, 549. (c) Koelle, U.; Kossakowski, J.; Boese, R. *J. Organomet. Chem.* **1989**, *378*, 449. (d) Loren, S. D.; Campion, B. K.; Heyn, R. H.; Tilley, T. D.; Bursten, B. E.; Luth, K. W. *J. Am. Chem. Soc.* **1989**, *111*, 4712. (e) Koelle, U.; Kang, B.-S.; Thewalt, U. *Organometallics* **1992**, *11*, 2893. (f) Koelle, U.; Rüther, Th.; Klaüi, W. *J. Organomet. Chem.* **1992**, *426*, 99. (g) Johnson, T. J.; Folting, K.; Streib, W. E.; Martin, J. D.; Huffman, J. C.; Jackson, S. A.; Eisenstein, O.; Caulton, K. G. *Inorg. Chem.* **1995**, *34*, 488.
11. (a) Lunder, D. M.; Lobkovsky, E. B.; Streib, W. E.; Caulton, K. G. *J. Am. Chem. Soc.* **1991**, *113*, 1837. (b) Johnson, T. D.; Huffman, J. C.; Caulton, K. G. *J. Am. Chem. Soc.* **1992**, *114*, 2725.
12. (a) Stewart, W. S.; Siddall, T. H., III. *Chem. Rev.* **1970**, *70*, 517. (b) Gansow, O. A.; Killough, J.; Burke, A. R. *J. Am. Chem. Soc.* **1971**, *93*, 4297. (c) Curran, D. P.; Tamine, J. *J. Org. Chem.* **1991**, *56*, 2746. (d) Nagashima, H.; Isono, Y.; Iwamatsu, S. *J. Org. Chem.* **2001**, *66*, 315.
13. (a) Sloigh, G. A. *Tetrahedron Lett.* **1993**, *34*, 6825. Also see: (b) Iwamatsu, S.; Kondo, H.; Matsubara, K.; Nagashima, H. *Tetrahedron* **1999**, *55*, 1687.
14. DFT calculations (B3LYP/6-31++G(d,p)//B3LYP/6-31G(d) level) were performed using Gaussian 98 package: *Gaussian 98*, Revision A.11; Gaussian Inc.: Pittsburgh, PA, 2001.
15. Stewart, J. J. P. *MOPAC2000: Lite*, version 1.1, Fujitsu Ltd: Tokyo, Japan, 2000.
16. Watanabe, Y.; Ando, T.; Kamigaito, M.; Sawamoto, M. *Macromolecules* **2001**, *34*, 4370.
17. An interesting difference between the ruthenium alkoxide **4a** and the diruthenium amidinate **3** as the polymerization catalyst is observed in the end group of the formed polymer. ATRP by **3** afforded the polymer having halogen atom at the end group, which undergoes reactivation by **3** to regenerate the active radical species at the polymer end. In contrast, post-polymerization of MMA from poly(MMA) ($M_n$=4000; $M_w/M_n$=1.2), which was obtained by the reaction shown in Table 5, entry 4 proceeded even at 25 °C to afford the poly(MMA) of $M_n$=40,000, but some of the starting macroinitiator remained. $^1$H NMR spectra of polymers formed by **4a** showed two broad signals at $\delta$ 6.15 and 5.42 ppm, which are assignable to the vinylic protons at the polymer end. These results suggest that the poly(MMA) formed by the present catalyst system contained both the terminal chloride (**F**) and the *exo*-methylene moiety (**G**). This may be attributed to the fact that **3** has a cationic species, which act as a Lewis acid, whereas **4d** is a metal alkoxide, which can behave as a base.


F G

18. (a) Kajiwara, A.; Matyjaszewski, K. *Macromolecules* **1998**, *31*, 3489. (b) Narita, M.; Nomura, R.; Endo, T. *Macromolecules* **1998**, *31*, 2774.
19. (a) Iura, T.; Matsubara, K.; Nagashima, H. In *The Reports of Advanced Material Study*, *Vol. 14*; Kyushu University: Fukuoka, 2000; p 119. (b) Nagashima, H.; Suzuki, A.; Iura, T.; Ryu, K.; Matsubara, K. *Organometallics* **2000**, *19*, 3579.
20. The reason why the polymerization of MMA proceeded at low temperature using poly(THF)-derived initiator **13** is not clear at present. We assumed that the polyether moiety of both the initiator **13** and the dormant chain might effectively stabilize the highly reactive ruthenium alkoxide **4a** with an oxophilic nature.
21. For the metal-catalyzed atom-transfer reactions, the redox mechanisms shown in Scheme 1 are often proposed. Although possible involvement of free radical chain processes cannot be completely excluded in the ATRC and ATRP reactions presented in this paper, the following points strongly support the redox mechanism. First, the same coordinatively unsaturated complex catalyzes the both ATRC and ATRP; this suggests that these reactions proceed through similar mechanisms. Second, free radical polymerization generally provides polymers with wide molecular weight distributions, and termination process is disproportionation (Ref. 22). In contrast, the ATRP presented in this paper achieves the production of polymers having a halogen atom end group with narrow $M_w/M_n$s; this strongly suggests interaction of the radical species at the polymer end with the metallic species leading to abstraction of the halogen atom from the M–X species by the polymer radical. As a consequence of the first and the second points, ATRC should also be promoted by the redox mechanism not involving the free radical chain process.
22. Kashiwagi, T.; Kitayama, T.; Masuda, E. *Macromolecules* **1986**, *19*, 2160.
23. Bryans, J. S.; Chessum, N. E. A.; Parsons, A. F.; Ghelfi, F. *Tetrahedron Lett.* **2001**, *42*, 2901.
24. Clark, A. J.; Battle, G. M.; Bridge, A. *Tetrahedron Lett.* **2001**, *42*, 4409.
25. SIR97: Altomare, A.; Burla, M.; Camalli, M.; Cascarano, G.; Giacovazzo, C.; Guagliardi, A.; Moliterni, A.; Polidori, G.; Spagna, R. *J. Appl. Crystallogr.* **1999**, *32*, 115.
26. Beurskens, P. T.; Admiraal, G.; Beurskens, G.; Bosman, W. P.; de Gelder, R.; Israel, R.; Smits, J. M. M. *DIRDIF99: The DIRDIF-99 program system*; Technical Report of the Crystallography Laboratory; University of Nijmegen: The Netherlands, 1999.
27. Cromer, D. T.; Waber, J. T. In *International Tables for X-ray Crystallography*, *Vol. 4*; Kynoch: Birmingham, England, 1974; Table 2.2 A.
28. *CrystalStructure 3.7.0: Crystal Structure Analysis Package*, Rigaku and Rigaku/MSC (2000–2005); 9009 New Trails Dr. The Woodlands, TX 77381 USA.
29. Watkin, D. J.; Prout, C. K.; Carruthers, J. R.; Betteridge, P.W. *CRYSTALS*; Chemical Crystallography Laboratory: Oxford, UK, 1996.